Molecular Crystals and Liquid Crystals Science and Technology. Section A. Molecular Crystals and Liquid Crystals

Publication details, including instructions for authors and subscription information:
http://www.tandfonline.com/loi/gmcl19

Highly Birefringent Nematic Liquid Crystals for Reflective STN Applications

Mark Goulding [a] , Volker Reiffenrath [b] & Harald Hirschmann [b]

[a] Merck NB-SC, UK, University of Southampton, Highfield, Southampton, SO17-1BJ, UK

[b] Merck KGaA, Liquid Crystals Division, 64271, Darmstadt, Germany

Version of record first published: 24 Sep 2006

To cite this article: Mark Goulding, Volker Reiffenrath & Harald Hirschmann (2001): Highly Birefringent Nematic Liquid Crystals for Reflective STN Applications, Molecular Crystals and Liquid Crystals Science and Technology. Section A. Molecular Crystals and Liquid Crystals, 364:1, 899-910

To link to this article: http://dx.doi.org/10.1080/10587250108025063

Mol. Cryst. and Liq. Cryst., 2001, Vol. 364, pp. 899-910
Reprints available directly from the publisher
Photocopying permitted by license only

Highly Birefringent Nematic Liquid Crystals for Reflective STN Applications

MARK GOULDING[a], VOLKER REIFFENRATH[b] and HARALD HIRSCHMANN[b]

[a]*Merck NB-SC, UK, University of Southampton, Highfield, Southampton, SO17–1BJ, UK and* [b]*Merck KGaA, Liquid Crystals Division, 64271, Darmstadt, Germany*

An important parameter of any LCD containing portable electronic device is a low power requirement. The reflective STN display mode offers a moderate to high information content display with low power consumption. One method to realise colour in this mode is to use a large retardation (dΔn) value in the cell. For a cell gap of 6 μm, and a retardation of ~1.5, a birefringence (Δn) of greater than +0.2 is necessary. To achieve such a value in an STN LC mixture, materials with broad nematic range, good solubility and a Δn value of <+0.25 are required.

A study of the *trans*-cyclohexyldifluorophenyltolane core structure was made and a large number of dialkyl, alkenyl-alkyl and alkoxy materials were synthesised and characterised. These materials possess low to moderate melting points, broad purely nematic mesophases, a high Δn and very good solubility in nematic LC hosts. They are suitable materials for inclusion in mixtures for colour reflective STN displays.

Keywords: Synthesis; tolane; nematic; birefringence; fluorosubstitution; alkenyl

INTRODUCTION

For portable datagraphic applications such as mobile phones, personal digital organisers, palmtop computers, personal and in-car navigation systems etc. the working life between battery changes or recharge can be maximised if the power consumption of the display is minimised. An effective way to do this is to remove or not use any display lighting, utilising the display in a reflective mode. The reflective colour STN ECB mode display[(1)] is one such display type. The display mode utilises a high dΔn value, achieved through a high Δn in the LC mixture, to achieve maximum contrast. Typically, this mode uses a cell gap of c. 6 μm and has a dΔn requirement in the LC layer of ~ 1.5. Therefore, Δn in the LC layer must be >+0.2. To achieve this in a typical broad

temperature range nematic LC mixture, it is desirable to use some mixture components with $\Delta n > +0.25$.

There are many different ways in which to produce a high value of Δn in a calamitic LC molecule. Extending the delocalised π electron system, which increases the anisotropy of molecular polarisability is one way to do this and many molecular designs have been realised[2-6].

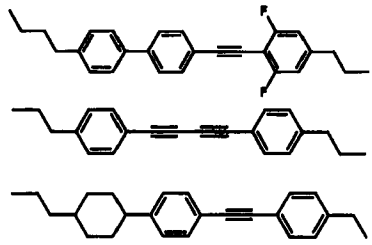

FIGURE 1 Tolane containing liquid crystals.

Incorporation of the diphenylacetylene (tolane) fragment into calamitic LC structures produces the extended π electron system necessary for a high Δn value [Figure 1]. Tolane LC materials are typically nematogenic and highly birefringent, but quite often they have high (100° C+) melting points and low solubility in nematic LC mixtures. Lateral fluorosubstitution can be used in LC material design to reduce melting points, depress the temperature of smectic phase formation and improve solubility[7]. "Forked" difluorosubstitution at certain positions in a tolane structure[2] can produce low melting, broad nematic phase materials. Several 1-((4-n-trans-cyclohexyl)-3,5-difluorophenyl)-2-phenylacetylene materials where n = n-C_3H_7 and m = F, OCF_3 etc. have been reported by Buchecker *et al.*[8]. In this paper, results are presented for the synthesis and characterisation of 1-((4-n-trans-cyclohexyl)-3,5-difluorophenyl)-2-phenylacetylene materials [Figure 2] with either alkyl, alkenyl, alkoxy or fluoro endgroups.

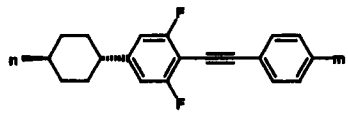

n = n-alkyl (C_1 - C_5) vinyl, 3-butenyl.

m = n-alkyl (C_1 - C_5), n-alkoxy (C_1 - C_2), F.

FIGURE 2 Generic structure of 1-((4-n-trans-cyclohexyl)-3,5-difluorophenyl)-2-phenylacetylene materials.

EXPERIMENTAL

Synthesis

Materials reported in this paper were synthesised according to the pathways shown [Figures 3 – 6]. Crude materials were purified by flash chromatography on Merck 40 – 63μm silica gel, eluting with hexane and recrystallising to >99.5% purity from ethanol. Materials were analysed for purity by reverse phase HPLC. ^{1}H NMR and GCMS confirmed the structure of the materials.

Mesophase analysis.

Transition temperatures of the materials were determined by controlled temperature polarising optical microscopy and confirmed by DSC. Heating and cooling runs at rates of 10°C min^{-1} under nitrogen atmosphere between – 50 & 250 °C with samples measured in closed lid aluminium pans were made. Mesophase type was assigned by visual comparison with known phase standards.

Measurement of virtual birefringence ($\Delta n_{VIRTUAL}$)

Refractive index measurements of planar aligned 10% w/w solutions of the test compound in Merck ZLI 4792 were made using an Abbé refractometer at 20 °C, using Na_D 589nm light. Δn was determined using $\Delta n = n_e - n_o$. $\Delta n_{VIRTUAL}$ was determined by extrapolation from the value for pure Merck ZLI-4792.

Measurement of virtual dielectric anisotropy ($\Delta\varepsilon_{VIRTUAL}$)

Dielectric constant ($\varepsilon_{parallel}$ and $\varepsilon_{perpendicular}$) measurements of 10% w/w solutions of the test compound in Merck ZLI 4792 were made by an electrical capacitative method. $\Delta\varepsilon$ was determined using $\Delta\varepsilon = \varepsilon_{parallel} - \varepsilon_{perpendicular}$. $\Delta\varepsilon_{VIRTUAL}$ was extrapolated from the value for pure Merck ZLI-4792.

Measurement of virtual elastic constant ratio ($K3/K1_{VIRTUAL}$)

Elastic constant (K3 and K1) measurements of 10% w/w solutions of the test compound in Merck MDA93-867 were made by an electrical capacitative method at 20°C. $K3/K1_{VIRTUAL}$ was determined by extrapolation from the value for pure Merck MDA93-867.

Measurement of virtual flow viscosity ($\eta_{20\ VIRTUAL}$)

Measurement of flow viscosity (η_{20}) of the materials in the nematic phase of 10% w/w solutions of the test compound in a nematic host mixture (Merck ZLI-4792) were made by the U-tube method at 20°C. $\eta_{20\ VIRTUAL}$ was determined by extrapolation from the value for pure Merck ZLI-4792.

Measurement of virtual rotational viscosity ($\gamma_{1\ VIRTUAL}$)

Measurement of rotational viscosity (γ_1) of the materials in the nematic phase of 10% w/w solutions of the test compound in a nematic host mixture (Merck ZLI-4792) were made by an electrical method using an Autronics LCCS at 20°C. $\gamma_{1\ VIRTUAL}$ was determined by extrapolation from the value for pure Merck ZLI-4792.

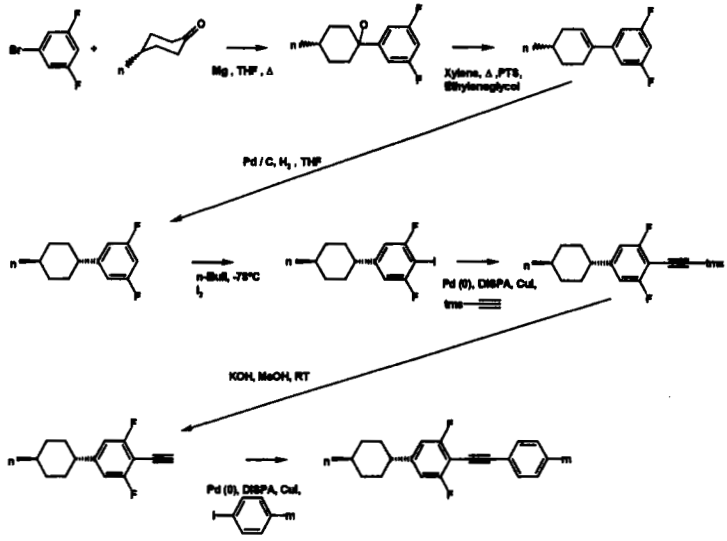

FIGURE 3 Synthesis of 1-((4-n-alkyl-*trans*-cyclohexyl)-3,5-difluorophenyl)-2-phenylacetylenes.

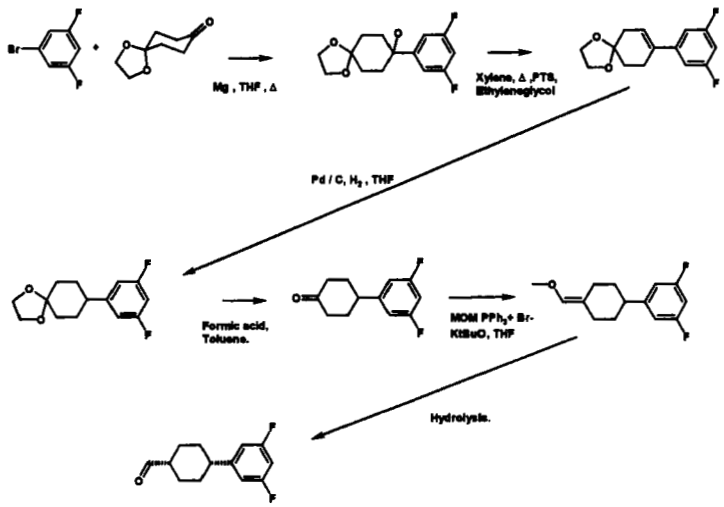

FIGURE 4 Synthesis of 4-(3,5-difluorophenyl) cyclohexanecarboxaldehyde).

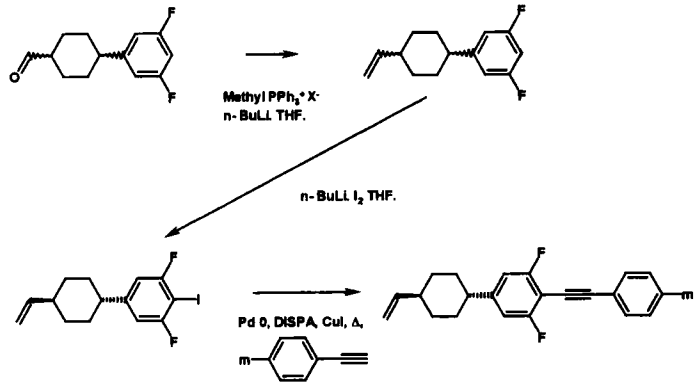

FIGURE 5 Synthesis of 1-((4-vinyl-*trans*-cyclohexyl)-3,5-difluorophenyl)-2-phenylacetylenes.

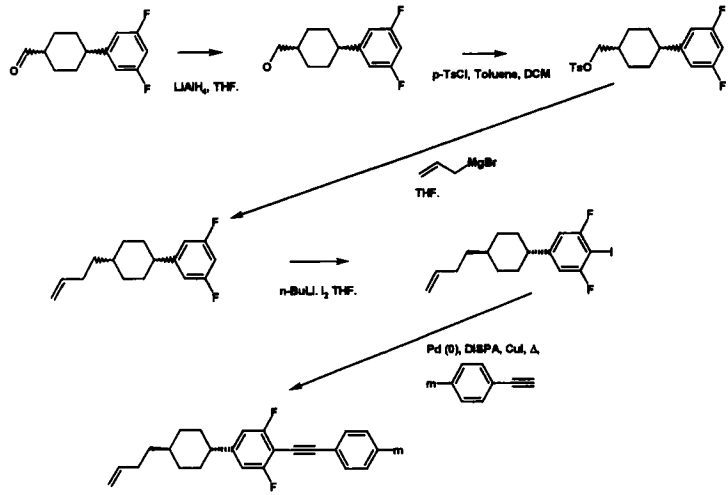

FIGURE 6 Synthesis of 1-((4-(3-butenyl)-*trans*-cyclohexyl)-3,5-difluorophenyl)-2-phenylacetylenes.

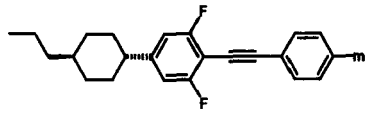

Compound	Mesophase behaviour / °C	$\Delta\varepsilon_{virtual}$	$\Delta n_{virtual}$	$\eta_{virtual}$	$K3/K1_{virtual}$	$\gamma_{1virtual}$
1. m = CH_3	C 102 N 189.8 I	3.64	+0.263	35	1.61	170
2. m = C_2H_5	C 64 N 181.2 I	3.15	+0.252	29	1.54	143
3. m = C_3H_7	C 55 N 192.8 I	3.63	+0.268	28	1.57	177
4. m = C_4H_9	C 63 N 178.0 I	3.08	+0.259	-	1.56	125
5. m = C_5H_{11}	C 55 N 182 I	3.78	+0.244	25	-	-
6. m = OCH_3	C 76 N 218.5 I	2.72	+0.280	38	1.71	274
7. m = OC_2H_5	C 92 N 224.2 I	3.33	+0.237	38	1.69	280
8. m = F	C 76 N 152 I	9.2	+0.231	22	-	-

TABLE 1 1-(4-(4-n-propyl-*trans*-cyclohexyl)-3,5-difluorophenyl)-2-phenylacetylene materials

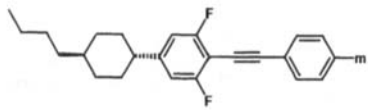

Compound	Mesophase behaviour / °C	$\Delta\varepsilon_{virtual}$	$\Delta n_{virtual}$	$\eta_{virtual}$	$K3/K1_{virtual}$	$\gamma_{1virtual}$
9. m = C_2H_5	C 64 N 167.4 I	3.03	+0.250	43	-	132
10. m = C_3H_7	C 63 N 174.2 I	2.67	+0.247	38	1.43	164
11. m = C_4H_9	C 83 N 165.6 I	2.62	+0.239	42	1.44	135
12. m = C_5H_{11}	C 58 N 167.3 I	2.51	+0.236	-	1.47	-

TABLE 2 1-(4-(4-n-butyl-*trans*-cyclohexyl)-3,5-difluorophenyl)-2-phenylacetylene materials.

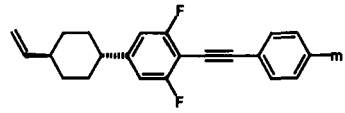

Compound	Mesophase behaviour / °C				K3/K1	
13. m = C_2H_5	C 79 N 173.9 I	2.54	+0.277	30	1.59	97
14. m = C_3H_7	C 69 N 183.0 I	2.28	+0.274	31	1.59	127
15. m = C_4H_9	C 48 N 166.2 I	2.38	+0.261	-	-	-
16. m = C_5H_{11}	C 67 N 173.2 I	2.32	+0.262	23	1.62	159
17. m = OCH_3	C 79 N 214.0 I	2.52	+0.298	48	1.78	205
18. m = F	C 76 N 142.3 I	7.45	+0.250	18	-	-

TABLE 3 1-(4-(4-vinyl-*trans*-cyclohexyl)-3,5-difluorophenyl)-2-phenylacetylene materials.

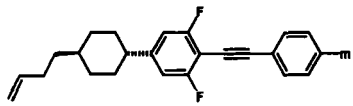

Compound	Mesophase behaviour / °C				K3/K1	
19. m = C_2H_5	C 75 N 176 I	2.92	+0.251	33	-	233
20. m = C_3H_7	C 57 N 183.9 I	2.86	+0.261	25	-	294
21. m = C_4H_9	C 68 N 174.3 I	2.51	+0.245	26	-	-
22. m = C_5H_{11}	C 52 N 177.5 I	2.27	+0.247	24	-	317
23. m = OCH_3	C 67 N 211.9 I	2.22	+0.284	37	-	-
24. m = F	C 88 N 147.4 I	7.47	+0.237	25	-	-

TABLE 4 1-(4-(4-(3-butenyl)-*trans*-cyclohexyl)-3,5-difluorophenyl)-2-phenylacetylene materials.

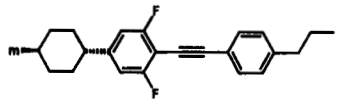

Compound	Mesophase behaviour / °C	$\Delta\varepsilon_{virtual}$	$\Delta n_{virtual}$	$\eta_{vir\,virtual}$	$K3/K1_{virtual}$	$\gamma_{1\,virtual}$
	C 66 N 160.8 I	3.3	+0.252	-	-	-
	C 69 N 183.0 I	2.28	+0.274	31	1.59	127
	C 55 N 192.8 I	3.63	+0.268	28	1.57	177
	C 79 N 221.2 I	3.67	+0.287	-	-	215
	C 63 N 174.2 I	2.67	+0.247	38	1.43	164
	C 57 N 183.9 I	2.86	+0.261	25	-	294

TABLE 5 1-(4-(4-(alkyl / alkenyl)-*trans*-cyclohexyl)-3,5-difluorophenyl)-2-(4-propyl)-phenylacetylene materials.

RESULTS AND DISCUSSION

Transition temperatures and extrapolated physical properties for materials **1 – 24** are reported in Tables 1 – 4. A comparison of alkyl and alkenyl materials is made in Table 5.

Mesophase behaviour

All of the synthesised materials show low to moderate melting points and broad nematic phases. All of the materials supercooled in the nematic phase to 30 – 40°C below their melting points. No smectic phases were observed by either DSC or temperature controlled optical microscopy in the supercooled temperature range. The data in Tables 1 – 5 show the effects of structural variation on melting point and mesophase behaviour.

If an examination of the melting points of materials **1 – 24** is made, some subtle effects are found. The variation of melting point for all of the materials is within 50°C, showing that the major influence on melting point is the core portion rather than the terminal substituents. The melting points are generally highest for the materials with the smallest terminal attachments, such as the methyl-substituted material **1**, the fluoro substituted materials **8**, **18** & **24** or the alkoxy substituted materials **6**, **7** & **17**. The size of a terminal substituent can affect the melting point of an LC material. It can act as a diluting and disrupting influence on the tendency of the rigid core portion of the molecule to pack in a solid crystalline lattice. From an examination of the data, the largest depression of melting point is found in the longer chain materials. There are some exceptions in the data, notably material **11**, which has two butyl substituents. The higher melting point in this instance may be as a result of a greater molecular symmetry. The materials with the highest melting points also possess the most polar substituents. This produces a larger molecular dipole moment, which may also enhance the stability of the crystalline lattice against melting. It is also noticeable that there is very little difference in the melting points of corresponding alkyl and alkenyl materials, e.g. materials **9 – 12** with materials **19 – 22**, suggesting that unsaturation in the terminal chain does not greatly effect the melting point.

The materials are all pure nematogens in both the enantiotropic and monotropic regions, irrespective of the terminal substituents. The principle reason for this is the lateral fluoro substituents in the core portion, which disrupt the close packing of the rigid core portions. If the aromatic cores are not able to interact closely, the tendency for smectic phase formation is greatly reduced. The explanation for this is usually that the presence of a lateral substituent causes the core portion to twist out of a more planar conformation, which decreases the smectogenicity[9].

If the data in Tables 1 – 5 is examined, it can be seen that structural variation has some effects on the nematic to isotropic transition or clearing point ($T_{[N-I]}$) for materials **1 – 24**. The classical "odd-even" effect of alkyl chain length[10] is observed in the materials with odd number homologues giving higher $T_{[N-I]}$ values. This effect is most magnified when a comparison of the 3,3- and 4,4-

dialkyl materials **3** & **11** is made; material **3**, the 3,3- homologue has a $T_{[N-I]}$ value 15°C higher and a nematic range almost 50°C broader than the material **11**, the 4,4- homologue material. The nature of the terminal chain also has an effect on the $T_{[N-I]}$ value. If a general comparison is made of the materials, it can be seen that the presence of an alkenyl group in the terminal chain increases the $T_{[N-I]}$ value by an average of 20°C. The position in the terminal chain of the alkenyl group also affects the $T_{[N-I]}$ value with the most pronounced increases appearing in the vinyl materials **13 – 18**. The trends observed in the alkenyl materials are in general agreement with the findings of Schadt *et al.*[11, 12] who made comprehensive investigations into the effects of alkenyl substitution in nematic LC materials.

Examination of the data also shows that for terminal fluorosubstituted materials **8**, **18** & **24**, the $T_{[N-I]}$ values are lower than for the alkyl or alkenyl analogues. The probable reason for this is a decreased length to breadth ratio for the molecule, which decreases the ability of a molecule to maintain calamitic liquid crystal mesophases. However, the use of an alkoxy terminal chain in place of an alkyl terminal chain (materials **6**, **7**, **17** & **23**) produces a marked increase in the $T_{[N-I]}$ values relative to the corresponding alkyl materials (average of 40°C increase). The explanation for this observed phenomena is that the alkoxy group, when in close proximity to the core portion of the molecule, increases the length of the rigid core portion, correspondingly increasing the molecular mesogenicity. The higher $T_{[N-I]}$ values for the vinyl materials **13 – 18** can be similarly explained.

Birefringence

All of materials **1 – 24** have similar virtual Δn values; in the region of +0.25 - +0.3, demonstrating that the terminal substituents have only a small effect in this core structure on Δn. However, some trends are observable. The highest values of Δn are seen in the methoxy compounds **6**, **17** & **23**. There are two possible reasons for this phenomenon. Firstly, attachment of the oxygen atom to the rigid core portion extends both the rigidity and the polarisability. If the polarisability is extended, it results in an increase of n_e, the parallel refractive index, which contributes to an increase on Δn. The second explanation is that as the $T_{[N-I]}$ value is maximised for the methoxy materials, the order parameter of the materials is increased at the temperature of virtual measurement. Δn, molecular polarisability in the three spatial directions of the molecule (α_{xx}, α_{yy} & α_{zz}) and the order parameter (S) are related by the following equation[13]:-

$$\Delta n \approx (\alpha_{zz} - (\alpha_{xx} + \alpha_{yy} / 2)) S$$

There is an exception to this phenomena with material **7**, an ethoxy chain material, which has a high clearing point but a lower Δn value. Correspondingly, the materials with terminal fluoro substitution have the lowest Δn and $T_{[N-I]}$ values, which is in agreement with the Maier – Saupe equation.

Comparing the two different classes of alkenyl materials, it is seen that only the vinyl materials **13 – 18** improve the Δn value relative to the alkyl materials. The optimum combination of highest Δn and $T_{[N-I]}$ value is observed in the vinyl materials, which combined with their shorter synthetic pathway compared to the 3-butenyl materials **19 – 24** makes them a superior choice for inclusion in STN LC mixtures.

Flow viscosity (η_{20}) & Rotational viscosity (γ_1)

The factors that affect viscosity in liquid crystals are complex and establishing structure-property relationships is more difficult than for other physical properties. Examination of the data for materials **1 – 24** shows some trends. The rigidity and polarity of the molecule influence γ_1. Examining the dialkyl materials **1 – 5 & 9 - 12**, there is a slight odd-even effect on the γ_1, but in the vinyl materials **13 – 18** there appears to be a more linear increase of γ_1 with increasing alkyl chain length. It can also be seen that in the alkoxy materials **6, 7, 17 & 23**, γ_1 is considerably increased relative to the alkyl materials. This may be due to the increased polarity of the O-atom and possible intermolecular interactions arising from it.

Dielectric anisotropy ($\Delta\varepsilon$) & Elastic Constant Ratio (K3/K1)

Examination of materials **1 – 24** shows that, with the exception of terminal fluoro substitution (materials **8, 18 & 24**) the nature of the terminal chain length and type has no effect on $\Delta\varepsilon$. All of the materials are slightly positively dielectric. The polar nature of the fluorine atom increases $\Delta\varepsilon$ by increasing $\varepsilon_{parallel}$. For STN LC applications, it is desirable to have a high K3/K1 ratio in the mixture to improve the electro-optical characteristic. K3 is the bend elastic constant and K1 is the splay elastic constant. These constants are a measure of the resistance to splay or bend distortions of the molecule in an electric field. From the data in tables 1 – 5, it can be seen that the butyl homologues (materials **9 – 12**) have lower K3/K1 ratios than other dialkyl materials and that alkenyl groups increase K3/K1. Also, the presence of the O-atom increases K3/K1 in alkoxy materials. Generally speaking, the more rigid vinyl materials have the best K3/K1 characteristic.

CONCLUSIONS.

From the data presented in Tables 1 – 4, it can be seen that materials **1 – 24** are all broad range, high Δn nematic liquid crystals with low to moderate melting points. The vinyl materials (**13 – 18**) have the best combination of high $T_{[N-I]}$ value, Δn, γ_1 and K3/K1 ratio. Although the synthetic pathway for the vinyl materials is more complex than for the alkyl materials, all of these material sub-classes are suitable for use in ECB STN mixtures for colour reflective applications.

ACKNOWLEDGEMENTS.

Hr. Haas, Hr. Heldmann, Hr. Mergner, Hr. Suess LC/FO/C Merck KGaA. & Kevin Adlem, Merck NB-SC, UK, for assistance with the analysis and characterisation of the materials.

References

[1] Mizuno, H., Fujita, N., Wakita, T., Otani, H., Yamaguchi, N., Naito, N., Sekime, T., Ogawa, T., presented at IDW 97.
[2] Reiffenrath, Volker; Hirschmann, Harald; Poster P3, *28th Freiburger Flussigkristalle Arbeitstagung*, 24–26/03/99.
[3] Grant, C., *Mol. Cryst. Liq. Cryst.*, **48**, 1978, 175, 178, 180.
[4] Takatsu, H.; Takeuchi, K.; Tanaka, Y.; Sasaki, M.; *Mol. Cryst. Liq. Cryst.*; **141**; 1986; 279–288.
[5] Wu, Shin-Tson, Margerum, J. D., Ho, M. S., Fung, B. M., Hsu, C. S., *Mol. Cryst. Liq. Cryst. Sci. Technol. Sect. A*, **261**(1), 1995, 79–86.
[6] Seils, Frank; Schadt, Martin; *Mol. Cryst. Liq. Cryst. Sci. Technol. Sect. A*, **260**, 1995, 127–138.
[7] Gray, G.W., Hogg, C. & Lacey, D., *Mol. Cryst. Liq. Cryst.*, **67**, 1981, 1 (and references contained therein.).
[8] Buchecker, Richard; Marck, Guy; Schadt, Martin, *Mol. Cryst. Liq. Cryst. Sci. Technol. Sect. A.*, **260**, 1995, 93–106.
[9] Gray, G.W., Hird, M. & Toyne, K. J, *Mol. Cryst. Liq. Cryst.*, **204**, 1991, 43.
[10] Gray, G.W., Harrison, K.J., Nash, J.A., *Electron. Lett.*, 1973, **9**, 130.
[11] Petrzilka, M., Buchecker, R. Schmeiderer, S-L., Schadt, M., Germann, A.; *Mol. Cryst. Liq. Cryst.*, **148**, 1987, 123 – 143.
[12] Kelly, S.M., *Liq. Cryst.* 20(5); 1996, 493–515.
[13] Maier, G., Saupe., *Z. Naturforschung*, 1959.